Microbes and Infectious Diseases 2024; 5(2): 463-478

Microbes and Infectious Diseases

Journal homepage: https://mid.journals.ekb.eg/

Original article

Evaluating the impact of seasonal Influenza virus: A comprehensive epidemiological forecast and analysis in Ghana from 2021 to 2023

Md Nurul Raihen[1]*, Md Mostak Ahammed[2], Sultana Akter[3]

1- *Department of Mathematics and Computer Science, Assistant Professor, Fontbonne University, St. Louis, MO, 63105, USA*
2- *Department of Statistics, Visiting Faculty, Grand Valley State University, Allendale, MI, 49401, USA*
3- *Sultana Akter, Teaching Assistant, MS in Statistics, Western Michigan University, Kalamazoo, MI, 49006, USA.*

ARTICLE INFO

Article history:
Received 26 December 2023
Received in revised form 20 January 2024
Accepted 4 February 2024

Keywords:
Seasonal influenza virus
Vaccination
Numerical approximation
Sensitivity analysis
Epidemic dynamics

ABSTRACT

Background: Infectious diseases are a leading cause of death and disability worldwide, so it is crucial to plan for their potential impact in order to implement an efficient response. Examining the seasonality and distribution of influenza viruses in Ghana, as well as susceptible demographic groups and circulating strains of the virus, were the objectives of this study. **Methods:** We worked with a modified version of the Susceptible-Exposed-Infectious-Recovered-Vaccinated (SEIR-V) transmission model to forecast the possible outcomes of the influenza pandemic in Ghana. Using the fourth-order Runge-Kutta method, we were able to get numerical simulations for changing the model parameters. We analyzed forecasts for the illness transmission rate β, vaccination rate ρ, and recovery rate γ on a daily and cumulative basis. The average fundamental reproduction number for the parameters β and γ was also rendered graphically. **Results:** We effectively forecasted the trajectory of influenza-related morbidity using our model, which paves the way for future approaches of controlling and monitoring the flu in our study area. In order to restrict the seasonal influenza, we have provided visual evidence that vaccinated patients and a quarantine in Ghana for at least the next 10 days are needed. It has been noted that the recovery rates of non-vaccinated patients and the vaccination rate work together to reduce the contagious disease. **Conclusion:** Using precise parameter approximations, theoretical epidemic analysis has proven to be an effective method for predicting and managing the spread of pandemics such as seasonal influenza virus. This model has been transformed into an epidemic model by adding the hospitalized-vaccination compartment for patients with confirmed infections to the SEIR-V model.

Introduction

The common symptoms of the human influenza virus include a hacking cough, a sore throat, a headache, muscle pain, dizziness, and coryza. Influenza appears to be similar to other respiratory virus illnesses unless laboratory testing proves different. Where it all began, influenza viruses belong to the family Orthomyxoviridae, which are members of the family of single-stranded ribonucleic acid (RNA) viruses. The influenza A, B, and C viruses are distinct from one another [1]. Influenza A and B viruses can produce pandemics, whereas type C viruses can cause a mild cold-like illness in humans. Flu A can infect a wide variety of

DOI: 10.21608/MID.2024.258309.1734
* *Corresponding author:* Md Nurul Raihen
E-mail address: *nraihen@fontbonne.edu*

mammals, including humans, as well as birds, both wild and domestic. Based on the genetic and antigenic features of their surface glycoprotein, influenza A viruses have been classified into nine neuraminidase (NA) subtypes and sixteen haemagglutinin (HA) subtypes. There is a vast array of possible combinations of the HA and NA proteins. Extensive human outbreaks have been associated with a handful of influenza A subtypes, namely H1N1 (H (Haemagglutinin type 1) and N (Neuraminidase type 1), H2N2 (H (Haemagglutinin type 2) and N (Neuraminidase type 2), and H3N2 (H (Haemagglutinin type 3) and N (Neuraminidase type 3) [2]. The current human influenza A subtypes that are circulating are H1N1, H3N2, and H7N9 (H (Haemagglutinin type 7) and N (Neuraminidase type 9) [3, 4, 5, 6].

According to multiple studies, a consistent set of symptoms was identified [7]. Conflicting evidence suggests that encephalitis, lethal pneumonia, and myositis are more common complications of influenza B infection [8]. Hospitalization rates are higher for children infected with influenza A because they are more likely to show severe symptoms, such as an unwell appearance and other signs and symptoms of the disease [9]. Based on the results of the microneutralization experiment, it has been concluded that neither infants nor adults are able to develop a cross-reactive humoral immune response to the pandemic virus by vaccination. This was found out by comparing human sera taken before and after seasonal flu vaccine administration [10, 11, 12].

In public health, mathematical modeling is crucial for understanding and predicting disease outbreaks. By mimicking the transmission of diseases, these models assess the consequences of various interventions [13]. With their help, we can streamline our data analysis, identify trends, and draw conclusions based on solid evidence. Health officials can utilize models like SEIR-V (Susceptible-Exposed-Infectious-Recovered-Vaccinated) to predict the future trajectories, which will help us better prepare for and react to diseases [14]. It is essential to have them in order to distribute vaccines, allocate resources, and set up control mechanisms. Public health professionals use mathematical modeling to gain valuable insights from raw data and reduce the impact of infectious diseases on communities [15].

Many developed regions of the world have a good understanding of the viruses that cause influenza-like illness (ILI) [16]. This data is critical for public health interventions and prevention programs to be effective. Conversely, neither the epidemiological knowledge of ILI nor the agents responsible for its etiology in developing countries are well-established. This lack of data makes it very difficult for many nations to implement effective public health interventions and preventative measures. Lack of data also makes it hard to create realistic models of pandemic influenza infections and to construct effective control measures [17]. Public health responses to ILI can be enhanced by conducting more research and surveillance to better understand the disease and how it spreads. This is particularly important in developing countries with incomplete epidemiological data [18].

Flu is one of the leading causes of respiratory infections in Ghana. In the past, the country has been hit hard by influenza pandemics. The 1918 Spanish flu pandemic is one example of this. In response to a highly pathogenic avian influenza A(H5N1) outbreak in 2007, virological surveillance for influenza-like illness (ILI) was created by the Noguchi Memorial Institute for Medical Research (NMIMR) and other international and local health organizations. A component of the Integrated Disease Surveillance and Response (IDSR) system, this monitoring was conducted by the Ghana Health Service (Ministry of Health) [19].

The National Influenza Centers (NICs) and other national influenza laboratories from 122 countries, regions, or territories supplied data to FluNet between November 13, 2023, and November 26, 2023 (as of 08/12/2023 06:22:56 AM UTC). During that period, the laboratories affiliated with the WHO GISRS examined more than 301,639 specimens. Out of 36,530 individuals who tested positive for influenza, 32,078 (or 87.8%) had influenza A and 4,861 (12.2%) had influenza B. The A(H1N1) pdm09 subtype had 21,327 cases (81.4%) while the A(H3N2) subtype had 4861 cases (18.6%). No less than 2,892 type B viruses belonged to the B/Victoria subgroup that could have their history traced [20].

As a result of the carefully placed sentinel sites across the country, influenza surveillance in Ghana covers a wide area. A complete picture of the influenza pandemic's spread can be created by utilizing this diverse set of locations, which includes

both civilian and military medical reception posts. Flu cases in Ghana tend to spike during the rainy season (April to October), indicating a seasonal pattern in the country's influenza cases. According to surveillance data collected between 2011 and 2019, the number of influenza cases was higher during these rainy months compared to the dry season (November to March). Several factors may contribute to the seasonal increase in influenza cases that occur just before or just after a rainstorm. A shift in human behavior, such as spending more time indoors, may contribute to the disease's spread. Additionally, weather changes brought on by the rainy season might make the flu virus more hospitable to survival and transmission. While 21,747 samples were tested for influenza-like illness (ILI), 3,429 samples were analyzed for severe acute respiratory illness (SARI) [18]. The influenza positive rates were highest in the 5–14 age group among both ILI and SARI. Fewer cases were reported in health centers during the dry season (November-March) in Ghana compared to the wet season (April-October). Although seasonal influenza occurs annually in Ghana, there has been no investigation into methods for predicting the accompanying monthly morbidity. The implementation of prediction-based early warning systems would substantially improve disease control, community engagement, and personal safety [21].

This study details the clinical presentation and socio-economic impact of 901 normally healthy children who visited the emergency room (ER) due to flu-like symptoms during the 2021–2022 and 2022–2023 flu seasons, and whose infections were confirmed by laboratory testing as influenza A (H1N1 and H3N2) or B. The purpose of this research was to increase the potential sample sizes and time frames for studying individual-level selection forces by making use of publicly available influenza virus consensus sequencing data from routine monitoring. At the consensus sequence level, new phenotypically relevant sequence variants should be readily apparent if individual positive selection successfully shapes influenza virus evolution [22]. Unfortunately, consensus sequences do not have the resolution that next-generation sequencing data does, making it impossible to describe within-host viral diversity or find potentially relevant denovo minority variations.

Thus, large-scale analyses of consensus sequencing data can tell us how individual-level positive selection plays a role in the seasonal influenza virus's evolutionary dynamics by revealing whether or not people with very different exposure histories to the virus exhibit any discernible patterns of substitution.

Objective

The key findings and innovative components of this study are as follows: (a) The non-negativity and boundedness of solution spaces are examined in this paper, along with a modified version of the Susceptible-Exposed-Infectious-Recovered-Vaccinated (SEIR-V) ordinary differential equation (ODE) model. (b) Based on a number of parameters, we have derived the disease-free equilibrium points and basic reproduction numbers that correspond to the required system of first-order ordinary differential equations (ODEs). (c) Numerical analysis has been conducted to investigate the effects of the disease's transmission and recovery rates on the dynamics of the seasonal influenza virus impact. (d) A plan is put forward to handle the seasonal influenza virus.

This study aims to examine the influenza epidemiology data set from Ghana, an African country. The article is structured according to the following outline: In section 3, we provide a context for the epidemiological and associated literature. Section 4 provides a detailed breakdown of the SEIR-V mathematical model. The seasonal influenza pandemic was also modelled using a compartmental approach, but this time they included a non-linear incidence rate [23, 24]. The solutions of non-negativity and boundedness are addressed in subsection 4.2 that follows. The point of equilibrium for the given model will be covered in section 5. The fundamental reproduction number can be obtained by following the straightforward computation shown in subsection 5.3. This is where we will find the "Results and Discussions" in section 6. Furthermore, parameter estimation for the system has been provided within the scope of subsection 6. Section 7 of this section also includes instances of numerical data with suitable visual representations. Section 8, the last section, presents the results and conclusions.

Mathematical model and formulation

The standard SIR model is used in the modeling of infectious diseases. This model enables the critical condition of disease development in a population to be determined given the overall

population size of that population. The most common demographic SIR form is characterized by [25].

$$\frac{dS}{dt} = \Lambda - \beta IS - \mu_1 S,$$
$$\frac{dI}{dt} = \beta IS - \gamma I - (\mu_1 + \mu_2)I, \quad (1)$$
$$\frac{dR}{dt} = \gamma I - \mu_1 I,$$

for any $t \in (0, \infty)$ subject to the initial conditions

$$S(0) = S_0, I(0) = I_0, \text{ and } R(0) = R_0,$$

and $N(t) = S(t) + I(t) + R(t)$ is the entire population at time t. Here, $S(t)$, $I(t)$, and $R(t)$, are the number of individuals in the susceptible, infectious and recovered compartments respectively at time t. The number of people who want to join the S class is Λ. The parameter β denotes the rate of disease transmission, γ is the rate of removal, μ_1 is the rate of normal death, and μ_2 is the rate of death only from infection. [25] contains the solution and thorough analysis of (1). It has been observed that the traditional SIR model is unable to investigate the situation of exposed and asymptotic individuals. This is a critical component in the propagation of the disease, particularly for pandemics of the SARS-CoV-2 and influenza virus types. As a result, it is absolutely necessary to take into consideration a more sophisticated model in order to monitor the behavior of asymptotically exposed class populations, as shown in **Figure 1**.

Proposed model

We propose the following SEIR-V (Susceptible-Exposed-Infectious-Recovered-Vaccinated Individuals) epidemic model to study the dynamics of influenza virus transmission in Ghana [26]. In the field of epidemiology, the SEIR-V model is a mathematical model that is utilized to investigate the diffusion of infectious diseases. This model is an extension of the SIR model, and it is utilized for modeling diseases that have a latent period before the infected person becomes infectiously contagious.

$$\frac{dS}{dt} = \Lambda - \beta \frac{SI}{N} - \rho SV - \mu S,$$
$$\frac{dE}{dt} = \beta \frac{SI}{N} - (\sigma + \mu)E,$$
$$\frac{dI}{dt} = \sigma E - (\gamma + \mu + \varepsilon)I, \quad (2)$$
$$\frac{dR}{dt} = \gamma I + \eta V - \mu R,$$
$$\frac{dV}{dt} = \rho SV - (\eta + \alpha + \mu)V,$$

with the initial conditions

$S(0) = S_0$, $E(0) = E_0$, $I(0) = I_0$, $R(0) = R_0$, $V(0) = V_0$,

and

$$N(t) = S(t) + E(t) + I(t) + R(t) + V(t),$$

where $N(t)$ is the total population size of the region at time t.

Here, $S(t)$, $E(t)$, $I(t)$, $R(t)$, and $V(t)$ represent the number of individuals in the susceptible, exposed, infected, recovered, and vaccinated compartments, respectively, at time t. **Table 1** provides an interpretation of the parameters that were used.

Now divide each differential equation in equation (2) by N and take S/N=s, E/N=e, I/N=i, R/N=r, V/N=v, and the parameter Λ/N=λ, then from equation (2), we get,

$$\frac{dS}{dt} = \Lambda - \beta si - \rho sv - \mu s,$$
$$\frac{dE}{dt} = \beta si - (\sigma + \mu)e,$$
$$\frac{dI}{dt} = \sigma e - (\gamma + \mu + \varepsilon)i, \quad (3)$$
$$\frac{dR}{dt} = \gamma i + \eta v - \mu r,$$
$$\frac{dV}{dt} = \rho sv - (\eta + \alpha + \mu)v,$$

with the initial conditions

$s(0) = s_0$, $e(0) = e_0$, $i(0) = i_0$, $r(0) = r_0$, $v(0) = v_0$,

and

$$s + e + i + r + v = n.$$

Solutions of non-negativity and boundedness

Theorem. Let $S = \{\boldsymbol{X} = (S, E, I, R, V) \in \Re \; such \; that \; X_k \geq 0 \; and \; \sum_{k=1}^{5} X_k \leq L\}$ be the closed set, then S is non-negative and bounded under the system (2), and solution $\boldsymbol{X}(t) \in S$ exists globally in time for the initial conditions $\boldsymbol{X}(0) \in S$.

Proof. Let Θ_k, where $k = 1, \ldots, 6$ be defined as follows

$$\Theta_k = \{\in S : X_k = 0 \text{ for } k = 1,2,3,4,5,6\},$$

and

$$\Theta_6 = \{\boldsymbol{X} \in S : \sum_{k=1}^{6} X_k = L\},$$

then it is obvious that $\partial S = \bigcup_{k=1}^{6} \Theta_k$.

In our study, we examine boundary segments, each labeled Θ_k, where $k = 1,2,3,4,5$. Associated with

each of these segments is an inward normal vector, referred to as $\boldsymbol{n}_k$. Each $\boldsymbol{n}_k$ is essentially a 6-dimensional vector, structured such that all components are zero except for the k^{th} component, which equals 1 and this can be represented as $n_k = \xi_k = (0,0,1,0,0,0)$, with the position of the '1' shifting based on the value of k and $n_6 = (-1,-1,-1,-1,-1,-1)$. Here, n signifies a vector as a positive linear combination of all the inward normals corresponding to the boundary segments. If we can show that $\boldsymbol{n} \cdot \boldsymbol{X}(t) \geq 0$, then our proof is complete. Thus, for $k = 1,2,3,4,5$ we get,

$\xi_1 \cdot \boldsymbol{X}' = \Lambda \geq 0$ for $\boldsymbol{X} \in \Theta_1$,

$\xi_2 \cdot \boldsymbol{X}' = \rho X_1 \geq 0$ for $\boldsymbol{X} \in \Theta_2$,

$\xi_3 \cdot \boldsymbol{X}' = \alpha X_2 \geq 0$ for $\boldsymbol{X} \in \Theta_3$,

$\xi_4 \cdot \boldsymbol{X}' = \beta X_1 + \sigma X_3 \geq 0$ for $\boldsymbol{X} \in \Theta_4$,

$\xi_5 \cdot \boldsymbol{X}' = \eta X_2 + \gamma X_4 \geq 0$ for $\boldsymbol{X} \in \Theta_5$,

Since $\sum_{k=1}^{6} X_k = L$, then we have,

$\frac{dN}{dt} = \Lambda - \mu N - \varepsilon X_4$,

Consequently, on Θ_6, where $N = L$, then we get,

$\xi_6 . \boldsymbol{X}' = -\Lambda + \mu L + \varepsilon X_4 \geq 0$.

Since S is positively invariant, our proof is complete.

Remark: The solution $\boldsymbol{X}(t) \in S$ exists for the close of the initial conditions $\boldsymbol{X}_0 \in S$.

Now we are going to develop a few fundamental results in the next section, which will be utilized throughout the rest of the analysis.

Stability and analysis of the model

Endemic equilibrium point (EEP)

An infectious disease's steady state in a population can be represented by its endemism equilibrium point, which is a crucial concept in epidemiology. The number of infected persons in a group stays constant throughout time, indicating that the illness is neither expanding nor dying out. This situation is called an endemic equilibrium point.

An essential factor in the development of the SEIR-V model was the presence of an endemic equilibrium point. For example, illness persistence and endemic equilibrium might occur in a population if the vaccination rate falls below a specific threshold.

In order to compute the point of endemic equilibrium of equation (3), we set

$\frac{ds}{dt} = \frac{dv}{dt} = \frac{de}{dt} = \frac{di}{dt} = \frac{dr}{dt} = 0$.

Then, we obtain the following system of equations:

$$\begin{aligned} &\Lambda - \beta si - \rho sv - \mu s = 0, \\ &\beta si - (\sigma + \mu)e = 0, \\ &\sigma e - (\gamma + \mu + \varepsilon)i = 0, \\ &\gamma i + \eta v - \mu r = 0, \\ &\rho sv - (\eta + \alpha + \mu)v = 0, \end{aligned} \quad (4)$$

By solving these equations in (4), we obtain the endemic equilibrium (EE),

$$\begin{aligned} s &= \frac{(\mu+\sigma)(\varepsilon+\gamma+\mu)}{\beta\sigma}, \\ e &= \frac{\Lambda\beta\sigma - \varepsilon\mu^2 - \varepsilon\mu\sigma - \gamma\mu^2 - \gamma\mu\sigma - \mu^3 - \mu^2\sigma}{\beta\sigma(\mu+\sigma)}, \\ i &= \frac{\Lambda\beta\sigma - \varepsilon\mu^2 - \varepsilon\mu\sigma - \gamma\mu^2 - \gamma\mu\sigma - \mu^3 - \mu^2\sigma}{\beta(\mu+\sigma)(\varepsilon+\gamma+\mu)}, \\ r &= \frac{\gamma(\Lambda\beta\sigma - \varepsilon\mu^2 - \varepsilon\mu\sigma - \gamma\mu^2 - \gamma\mu\sigma - \mu^3 - \mu^2\sigma)}{\beta\mu(\mu+\sigma)(\varepsilon+\gamma+\mu)}, \\ &0, \end{aligned} \quad (5)$$

Therefore, endemic equilibrium point (EEP) is

$$E = \begin{pmatrix} \frac{(\mu+\sigma)(\varepsilon+\gamma+\mu)}{\beta\sigma}, \frac{\Lambda\beta\sigma - \varepsilon\mu^2 - \varepsilon\mu\sigma - \gamma\mu^2 - \gamma\mu\sigma - \mu^3 - \mu^2\sigma}{\beta\sigma(\mu+\sigma)}, \\ \frac{\Lambda\beta\sigma - \varepsilon\mu^2 - \varepsilon\mu\sigma - \gamma\mu^2 - \gamma\mu\sigma - \mu^3 - \mu^2\sigma}{\beta(\mu+\sigma)(\varepsilon+\gamma+\mu)}, \\ \frac{\gamma(\Lambda\beta\sigma - \varepsilon\mu^2 - \varepsilon\mu\sigma - \gamma\mu^2 - \gamma\mu\sigma - \mu^3 - \mu^2\sigma)}{\beta\mu(\mu+\sigma)(\varepsilon+\gamma+\mu)}, 0 \end{pmatrix}. \quad (6)$$

The next step is to demonstrate the consequences of the fundamental reproduction number and examine the stability of the equilibrium points.

Diseases free equilibrium analysis

An important idea in the study of infectious diseases is the disease-free equilibrium. It sheds light on the circumstances that allow for the complete eradication of a disease from a population. We can forecast how an epidemic will behave in the long run and assess the efficacy of various management strategies by studying the stability of the disease-free equilibrium.

Consider the disease free equilibrium is $E_0 = \left(\frac{\Lambda}{\mu}, 0,0,0,0\right)$, and the vaccination-only equilibrium is $V_0 = \left(\frac{\alpha+\eta+\mu}{\sigma}, 0,0, \frac{\eta(\Lambda\sigma-\alpha\mu-\eta\mu-\mu^2)}{(\mu\sigma(\alpha+\eta+\mu))}, \frac{\eta(\Lambda\sigma-\alpha\mu-\eta\mu-\mu^2)}{(\sigma(\alpha+\eta+\mu))}\right)$.

Then we express the Jacobian matrix of the system equation (3) as

$$J = \begin{bmatrix} -\beta i - \mu - \rho v & 0 & -\beta s & 0 & -\rho s \\ \beta i & -\mu - \sigma & \beta s & 0 & 0 \\ 0 & \sigma & a & 0 & 0 \\ 0 & 0 & \gamma & -\mu & \eta \\ \rho v & 0 & 0 & 0 & e \end{bmatrix},$$

where $a = -\varepsilon - \gamma - \mu$, and $e = \alpha - \eta - \mu + \rho s$.

We can now compute the Jacobian matrix J at E_0, that is,

$$J_{E_0} = \begin{bmatrix} -\mu & 0 & -\frac{\Lambda\beta}{\mu} & 0 & -\rho s \\ 0 & -\mu - \sigma & \frac{\Lambda\beta}{\mu} & 0 & 0 \\ 0 & \sigma & a & 0 & 0 \\ 0 & 0 & \gamma & -\mu & \eta \\ \rho v & 0 & 0 & 0 & b \end{bmatrix},$$

where $b = \frac{\Lambda\rho}{\mu} - \alpha - \eta - \mu$.

Now solving the characteristics equation, we get,

$\lambda_1 = -\mu$, $\lambda_2 = \frac{\Lambda\rho-\alpha\mu-\eta\mu-\mu^2}{\mu}$, $\lambda_3 = \frac{-\varepsilon\mu-\gamma\mu-2\mu^2-\mu\sigma-\sqrt{4\Lambda\beta\mu\sigma+C}}{2\mu}$, and

$\lambda_4 = \frac{-\varepsilon\mu-\gamma\mu-2\mu^2-\mu\sigma+\sqrt{4\Lambda\beta\mu\sigma+C}}{2\mu}$

where $C = \varepsilon^2\mu^2 + 2\varepsilon\gamma\mu^2 - 2\varepsilon\mu^2\sigma + \gamma^2\mu^2 - 2\gamma\mu^2\sigma + \mu^2\sigma^2$.

The values of the model parameters have a significant impact on the stability of the disease-free equilibrium point. An epidemic could break out under such circumstances if any of the eigenvalues have a positive real portion, indicating that the equilibrium is unstable. Therefore. λ_1 is stable (negative real part), λ_2 can be either stable or unstable, depending on the parameter values. If $\Lambda\rho > \alpha\mu + \eta\mu + \mu^2$, it will have a positive real part, indicating instability, λ_3 stability depends on the sign of their real parts. If the term inside the square root is less than the square of the other terms, they may have negative real parts and thus be stable. If not, they may be unstable, similarly for λ_4.

Basic reproduction number

The concept of the basic reproduction number, denoted as $\mathcal{R}_0$, holds a pivotal role in the field of epidemiology, particularly in the context of infectious disease modeling and threshold analysis. This fundamental parameter has a rich historical lineage, with its origins rooted in the groundbreaking contributions of eminent scientists such as Alfred Lotka and Ronald Ross. Alfred Lotka's pioneering work in mathematical biology laid the groundwork for understanding population dynamics, providing valuable insights into the potential for disease spread. On the other hand, Sir Ronald Ross's pioneering research on malaria transmission not only earned him a Nobel Prize but also advanced our comprehension of how infectious diseases can propagate within populations. These foundational contributions set the stage for the formalization and application of $\mathcal{R}_0$ by George MacDonald in 1952, marking a crucial milestone in the field of modern epidemiology [27].

The basic reproduction number, often referred to as the basic reproductive ratio or, occasionally, the basic reproductive rate, is a key parameter in epidemiological research. Its primary function is to assess whether an infectious disease has the potential to accelerate through a population. The importance of $\mathcal{R}_0$ lies in its role as a threshold parameter, determining the fate of an infectious disease outbreak within a community. As described in the literature, two critical scenarios emerge:

Theorem [28].

1. when $\mathcal{R}_0 < 1$, it signifies that the disease is unlikely to cause an epidemic and will likely die out.

2. while an $\mathcal{R}_0 > 1$ indicates the potential for an epidemic to occur, or for the disease to persist within the population.

The fundamental reproduction number $\mathcal{R}_0$ can be calculated analytically in the setting of the considered model, which includes the disease-free equilibrium (DFE) expressed as $(S_0, V_0, E_0, I_0, R_0) \equiv (\frac{\Lambda}{\mu}, 0,0,0,0)$. As previously shown in studies [25, 26, 29], this is performed using a well-established strategy known as the next-generation matrix method.

The following relation $\mathcal{R}_0 = \lambda(FV^{-1})$, where denotes the spectral radius of the matrix FV^{-1} [25, 26, 29], is the key to determining $\mathcal{R}_0$. This mathematical technique precisely quantifies influenza virus potential for transmission throughout a population. It gives a fundamental

understanding of the disease's dynamics and impact, giving researchers and policymakers vital insights into how the virus may spread.

For our SEIR-V model, let

$$\begin{bmatrix} 0 & \beta \\ 0 & 0 \end{bmatrix},$$

and

$$V = \begin{bmatrix} \sigma + \mu & 0 \\ -\sigma & \gamma + \mu \end{bmatrix}.$$

Here, F captures the production of new infections from the 'Infectious' compartment influencing both 'Susceptible' and 'Vaccinated' individuals (though we focus on 'Susceptible' for the NGM), and V captures the transition rates out of the 'Exposed' and 'Infectious' compartments, and other critical characteristics that improve our understanding of the progression of the infection.

Therefore, the inverse of V, we get

$$V^{-1} = \begin{bmatrix} \frac{1}{\sigma+\mu} & 0 \\ \frac{\sigma}{(\sigma+\mu)(\gamma+\mu)} & \frac{1}{\gamma+\mu} \end{bmatrix}.$$

The NGM is then calculated as FV^{-1}. The largest eigenvalue of this matrix gives the basic reproduction number $\mathcal{R}_0$. This calculation involves matrix multiplication and finding the inverse of matrix V, followed by computing the eigenvalues of the resulting matrix. So, we have

$$|FV^{-1} - \kappa I| = \begin{vmatrix} \frac{\beta\sigma}{(\sigma+\mu)(\gamma+\mu)} & 0 \\ 0 & 0 \end{vmatrix} = 0.$$

Therefore, the spectral radius of FV^{-1} is

$$\mathcal{R}_0 = \lambda(FV^{-1}) = \frac{\beta\sigma}{(\sigma+\mu)(\gamma+\mu)}. \qquad (7)$$

Estimation of parameters

A numerical solution to a first-order ordinary differential equation (ODE) is used to predict the disease's transmission throughout a population in this study. Because of its outstanding precision and reliability, the fourth-order Runge-Kutta method (RK4), which is implemented in Python, is utilized in this work to solve such ordinary differential equations (ODEs). To provide a true representation of the population and illness metrics, it is crucial to mention that all variables and parameters in this population model are non-negative by definition.

In order to get the model's predictions in line with the real data, fitting techniques like the least-squares method, which is improved by Latin hypercube sampling, are used to calibrate the parameters. If we want the model to capture the dynamics of diseases in the actual world, we need to go through this procedure. In this calibration, the Python approach is crucial because it finds the best values for the model parameters, which include infection rates, vaccination rates, recovery rates, and other disease-specific characteristics. The study's future numerical simulations are based on the ideally estimated parameters, which are reported in **Table 1**. These parameters are important to the model's fidelity. The RK4 algorithm for solving first-order differential equations is presented in **Algorithm 1**.

Applications and numerical analysis

Using the fourth-order Runge-Kutta method, we attempt to solve the nonlinear differential system given by equation (2) in this work. **Table 2** shows the parameter settings that formed the basis of our analysis. These values were derived from previous research [30, 31]. The models were run in Python with a world population of 5.50 billion approximately. Our model's parameters are fine-tuned to a rate per 1,000 people every day.

Parameter estimates for the world's population are presented in **Table 2**.

Figure 2 displays the fractions of various demographic groups throughout time, illustrating the results of numerical simulations. Blue represents those who are susceptible, yellow those who have been exposed, red those who have been infected, cyan those who have been vaccinated, and green those who have recovered. The simulation shows that the number of sensitive individuals is reducing with time, which means that more and more people are getting exposed to the virus and getting infected. Based on this pattern, a rapid breakout could be imminent. The recovery rate is not proportional to the rise in the number of infected and vaccinated patients, which is an intriguing observation. When comparing this group to the others, it becomes clear. Equation (7) shows that the basic reproduction number $\mathcal{R}_0$ is 0.00000478, which is less than 1, based on the parameters given in **Table 2**. This means that an epidemic is less likely to occur under these conditions. Nevertheless, keep in mind that the values picked at random for γ and ρ make these results not definitive. A thorough sensitivity analysis of the model is required when trying to predict with any degree of accuracy how these

parameters would change and how they would influence the model's stability.

Sensitivity analysis

One important step in using modeling to understand the dynamics of infectious diseases is to do a sensitivity analysis. With this information, we can better understand how different parameter values affect the course of the disease and maybe develop ways to stop it in its tracks. Applying the model parameters listed in [32] with the values from **Table 2**, we will now conduct a sensitivity analysis of the fundamental reproduction number, $\mathcal{R}_0$, in respect to these parameters. As seen in equation (7), we may see this in action by determining $\mathcal{R}_0$'s sensitivity index relative to the parameter β.

Thus,

$$\zeta_{\beta}^{\mathcal{R}_0} = \frac{\partial \mathcal{R}_0}{\partial \beta} \times \frac{\beta}{\mathcal{R}_0},$$
$$= \frac{\sigma}{(\sigma+\mu)(\gamma+\mu)} \times \frac{(\sigma+\mu)(\gamma+\mu)}{\sigma} = 1.$$

Also, we determine the total sensitivity index in a similar fashion,

$$\zeta_{\Lambda}^{\mathcal{R}_0} = 0,$$
$$\zeta_{\rho}^{\mathcal{R}_0} = 0,$$
$$\zeta_{\mu}^{\mathcal{R}_0} = -\frac{\sigma+\gamma+2\mu}{(\sigma+\mu)(\gamma+\mu)} = -\frac{1}{\gamma+\mu} - \frac{1}{\sigma+\mu}$$
$$= -1.4,$$
$$\zeta_{\eta}^{\mathcal{R}_0} = 0,$$
$$\zeta_{\sigma}^{\mathcal{R}_0} = -\frac{\gamma+\mu}{(\sigma+\mu)(\gamma+\mu)} = -\frac{1}{\sigma+\mu} = -0.8,$$
$$\zeta_{\gamma}^{\mathcal{R}_0} = -\frac{\sigma+\mu}{(\sigma+\mu)(\gamma+\mu)} = -\frac{1}{\gamma+\mu} = -0.6,$$
$$\zeta_{\alpha}^{\mathcal{R}_0} = 0.$$

Here are the outcomes that follow from the index analysis: From $\zeta_{\beta}^{\mathcal{R}_0} = 1$, it is clear to us that a 10% increase in the exposure rate β would lead to a 10% increase in, which might cause an epidemic to ensue. Alternatively, β were to reduce by 10%, there would be a corresponding decrease in, which would help control the sickness of seasonal flu virus. Accordingly, controlling the spread of infection requires lowering the exposure rate. The World Health Organization and other government agencies have called for social distance and house quarantine as public health measures to combat the influenza virus, and this reasoning supports their recommendations.

In addition to that, $\zeta_{\sigma}^{\mathcal{R}_0}$ implies that the value is negative, we may deduce that a 10% increase in σ results in an 8% decrease in $\mathcal{R}_0$. In order to stop the spread of the disease, it is necessary to vaccinate the affected individual more often. Similarly, $\zeta_{\mu}^{\mathcal{R}_0}$, and $\zeta_{\gamma}^{\mathcal{R}_0}$ both values are negative, so in order to prevent the influenza virus, it is necessary to raise both the recovery rate of non-vaccinated individuals and the death rate as a result of infected, as raising the parameters has a negative influence on $\mathcal{R}_0$.

Case study: Results and Discussion

During the 32nd week of epidemiology, virological data was provided for analysis by 18 African countries. Out of 1,026 specimens collected during week 32, 1,011 were tested for influenza in Ghana (Data source: https://www.who.int/tools/flunet).

A total of 132 specimens, or 13.06%, tested positive for influenza virus in Epiweek 32; 81 of these specimens were influenza A and 51 were influenza B. Influenza A (H1N1) pdm09, influenza A (H3), influenza A (subtyping not conducted), influenza B (lineage not specified), influenza B (Victoria), and 38 instances of influenza A (H1N1) pdm09 were among the influenza viruses found.

From weeks 1 to 32, the WHO AFR influenza laboratory network measured 67,285 specimens; 5,319 of them, or 7.91%, proved positive for influenza virus. The infection-related mortality rate in Ghana is significantly more than the global average, standing at 6.7% as of April 10, 2023. Inadequate testing kits and treatment facilities could make the nation's response to a pandemic more challenging.

Based on the country's current situation, we estimated the parameters in **Table 3** after evaluating the scenario using the model provided in equation (3). According to **Table 3**, the reproduction number $\mathcal{R}_0$. is 13.4 >1, which is indicative of a severe and extensive problem. The continuous nature of the event and the paucity of testing sites across the country might often make actual data unavailable, resulting in the estimation of few parametric values for computation [33, 34].

There has been a dramatic decline in the susceptible population and a corresponding increase in the infected population, as seen in **Figure 3**. It is also possible to see, with some effort, that the number of infected individuals reaches a maximum at about 20 days and then starts to fall. The amount of the isolated (cyan) and recovered (magenta) populations is also fairly tiny when compared to the

infected population curve. We can confidently say that the virus's spread will be rapid. A high number of infected individuals in a very short length of time could result from the situation rapidly spiraling out of control if adequate precautions are not implemented which is why we need to act immediately to mitigate its effects.

The virological data provided by the WHO is displayed in **Figure 4**. **Figure 4** shows that there were 1,011 positive results for influenza testing out of 1,026 specimens collected in Ghana. In Epiweek 32, 132 out of 1011 specimens tested positive for influenza virus, accounting for 13.06% of the total. Of them, 81 were influenza A types and 51 were influenza B kinds. **Figure 4** also shows that out of the total number of influenza viruses discovered, 38 were influenza A (H1N1) pdm09, 35 were influenza A (H3), 8 were influenza A (subtyping not conducted), 31 were influenza B (lineage not determined), and 20 were influenza B (Victoria). Between weeks 1 and 32, the AFR influenza laboratory network of the World Health Organization screened 67,285, or 67,563 specimens, for the influenza virus. Out of these, 5,319 tested positive, giving a positivity rate of 7.91%.

We can proceed with our analysis after we complete the phase where we just examine the effect of by selecting $\beta = 0.9234$ (representing 92% of the infected population), $\beta = 0.7089$, and then up to $\beta = 0.1$. Increasing the number of testing and treatment facilities is the only way to decrease the infected population, which can be achieved by increasing the vaccination rate, as demonstrated by the curves in **Figure 5**.

The lack of an operational healthcare system in Ghana means that a lot of information is missing. The government has not been able to provide a sufficient amount of testing spaces, but they are still trying to find a solution. Therefore, it is a tough undertaking just to identify sick people, much less isolate as well as vaccinate them. Also, this highly populous nation has inadequate treatment facilities and equipment, so a huge number of diseases happening at once could have disastrous consequences. Isolating most of them gets increasingly challenging. We have determined that increasing the pace of vaccination, the number of treatment facilities, and testing can contain the epidemic by analyzing the curves in **Figure 5**.

Figure 6 shows the results of a 160-day SEIRV model simulation, showing how the vaccinated population grows under five different vaccination rates (ρ) from 0.05 to 0.459 (representing 46% of the vaccinated population). A more quick and broad vaccination effort is indicated by higher ρ values, which cause the peaks of each curve to be earlier and larger, reflecting the greatest reach of vaccination at different rates. Post-peak drops indicate that the number of people at risk is decreasing or that vaccine immunity is starting to wear off. The graphic comparison highlights the significance of effective vaccine distribution in reducing the transmission of infectious illnesses and the crucial role that vaccination speed plays in public health outcomes.

Given all parameters from **Table 3** set to fixed levels, **Figure 7** illustrates that when the non-vaccinated/natural recovery rate grows, the number of infected populations is declining. Here, the natural recovery rate may be thought of as the population's inherent immune system. A high value may suggest a positive outcome in this epidemic if the majority of the infected individuals have a strong immune system, either naturally or intentionally generated (by medicine or vaccine). On the other hand, people whose immune systems aren't as strong take more time to get well. Thus, educating the public on the importance of a balanced diet, regular exercise, and mental wellness is a crucial step in containing the seasonal flu-virus.

Based on our findings, it seems that additional diagnostic and treatment facilities for the affected population, social isolation of the community, and improved natural immunity or vaccine could be necessary to contain the seasonal influenza virus.

Table 1. Description of model parameters

Notation	Interpretations
Λ	Birth rate
β	Transmission rate from S to I class
ρ	Vaccination rate of S population
μ	Natural death rate
σ	Rate of progression from E to I
γ	Recovery rate from I class
η	Loss of vaccine-induced immunity rate
α	Diseases-induced death rate
N	Total population

Table 2. Initial conditions and parameters for the global

Parameters	Value	References
Λ	60	[30]
β	0.00001625	estimated
ρ	0.005	estimated
μ	0.6725	[31]
σ	0.578	estimated
γ	0.8975	estimated
η	0.01	estimated
α	0.0000025	estimated

Table 3. Initial conditions and parameters for Ghana

Parameters	Value	References
Λ	2.7×10^{-3}	[30]
β	2	estimated
ρ	1.54×10^{-6}	estimated
μ	0.0148	[30]
σ	1.02	[31]
γ	0.132	estimated
η	0.084	[30]
α	1.02	[31]

Figure 1. A diagrammatic representation of the transmission dynamics presents in the SEIR-V model

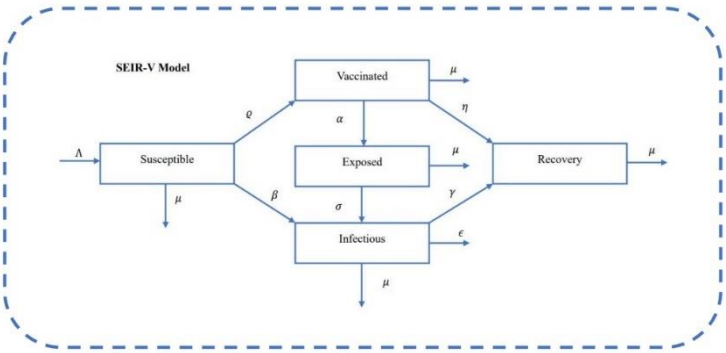

Figure 2. Over time, the dynamics of various population groups susceptible, exposed, infected, vaccinated, and recovered are represented through distinct curves. The blue line (Susceptible) decreases sharply at the beginning, indicating a rapid reduction in the number of individuals who are susceptible to infection. The yellow line (Exposed) shows the number of individuals who have been exposed to the infection and are in the incubation period. The red line (Infected) represents individuals who are actively infected and can transmit the disease to others; this peaks and then declines as the individuals either recover or die. The green line (Recovered) increases over time, indicating individuals who have recovered from the infection and have gained immunity. The cyan line (Vaccinated) shows the portion of the population that has been vaccinated over time. All data points for these curves are derived from the values presented in **Table 2**.

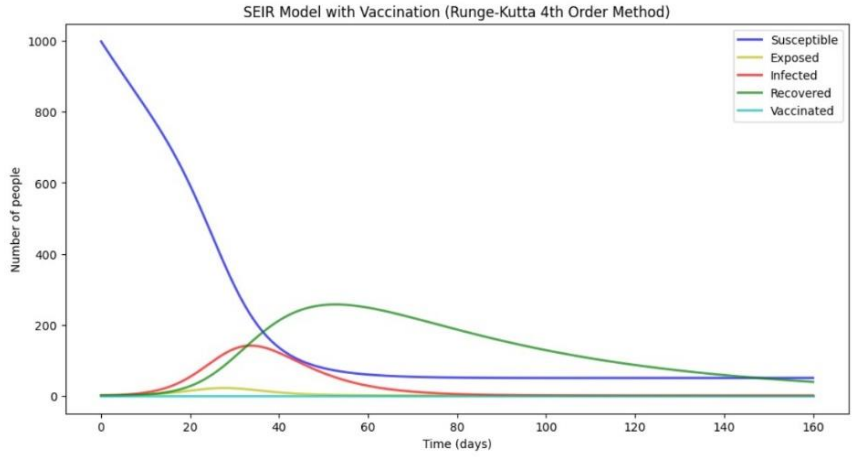

Figure 3. Population dynamics in Ghana, including susceptible, exposed, infected, vaccinated, and recovered states, as experienced across time. Various shades of hue denote distinct demographics: The colors blue, yellow, red, cyan, and green represent different stages of infection and recovery.

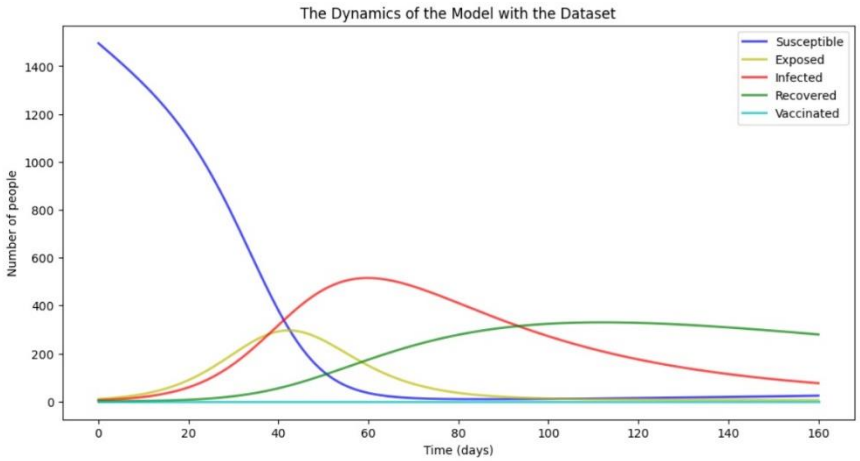

Figure 4. Epicurve of influenza cases in WHO AFR countries, areas, and territories by influenza type from the WHO African region (WHO AFR) provided virological data.

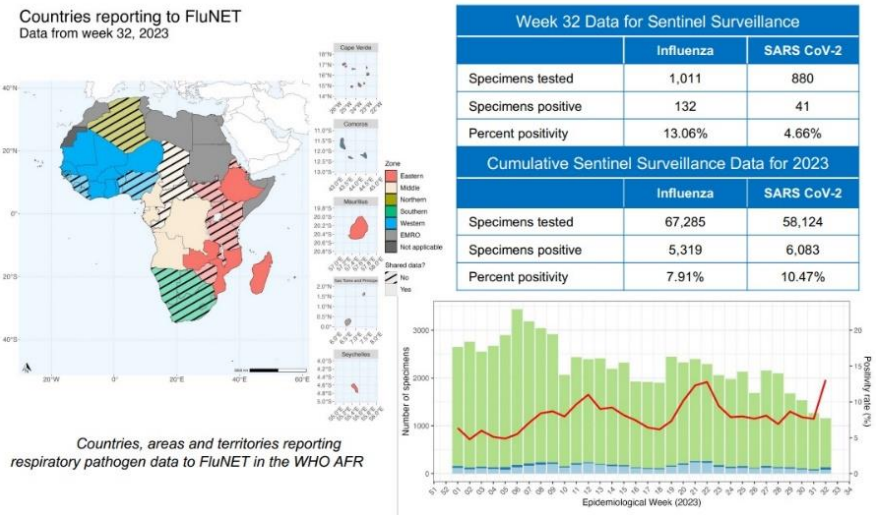

Figure 5. The dynamics of the infected population with and without increased vaccination, with purple indicating a large number of infected individuals becoming vaccinated and red indicating no vaccination.

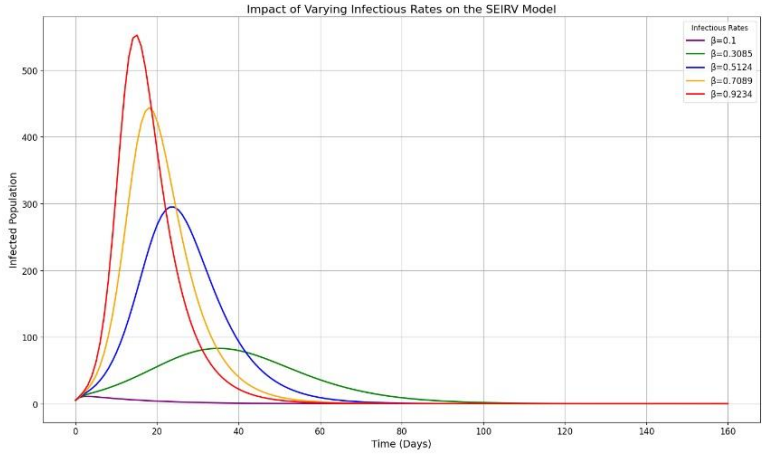

Figure 6. The dynamics of the vaccinated population demonstrate that greater rates lead to more rapid and extensive vaccination coverage in a population.

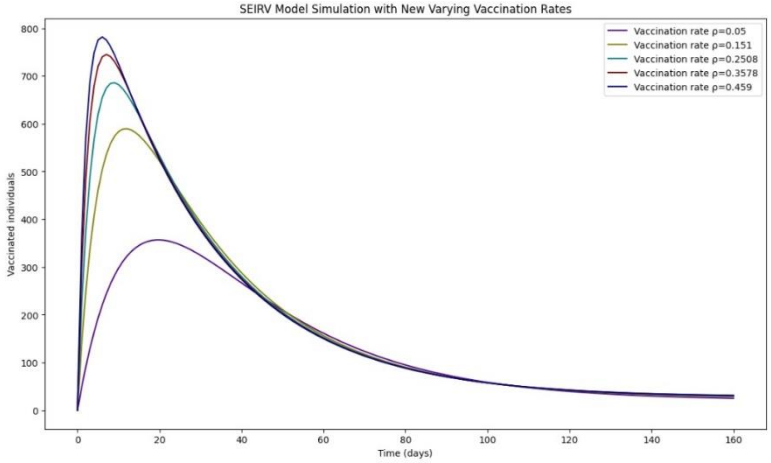

Figure 7. The rate of recovery of the diseased population according to γ dynamics. Potential effects on the seasonal flu situation as a result of a faster recovery rate in the non-vaccinated population are shown in this graphic.

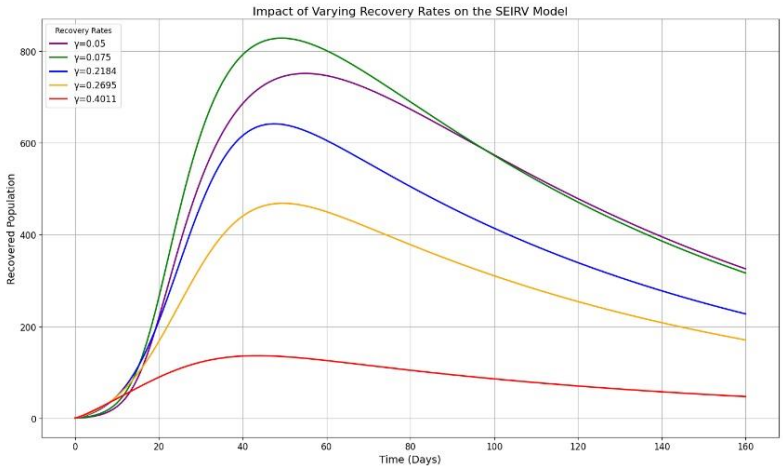

Algorithm 1. Introduces the RK4 algorithm, which is used to solve differential equations of first order.

Algorithm 1: RK4 Algorithm

Data: Consider, IVP

$$\begin{cases} \frac{dy}{dt} = F(x,y), \forall x \in [a,b] \\ y(a) = y_0 \end{cases}$$

Time step:$t_i = t_0 + ih$, where h is the time step size

Result: Numerical solution, y

Initialize: $s_0 = a$
for $i = 1 : I$ **do**
  The next time space t_{i+1}
  Compose $y(t_{i+1})$
  Compute
  if $i = 1$ **then**
    Compute $K_1 = h * F(t_i, s_i)$,
    $K_2 = h * F(t_i + \frac{n}{2}, s_i + \frac{K_1}{2})$,
    $K_3 = h * F(t_i + \frac{n}{2}, s_i + \frac{K_2}{2})$,
    $K_4 = h * F(t_i + n, s_i + K_3)$
  Update
  $s_{i+1} = s_i + \frac{1}{6}[K_1 + 2K_2 + 2K_3 + K_4]$
Solution for y

Discussion

A highly successful method for predicting and controlling the condition of viral infections like seasonal influenza can be achieved by theoretical epidemic analysis, provided that the parameters can be approximated correctly. We modified the SEIR-V model to reflect an epidemic by including the hospitalized-vaccination compartment for patients who have been diagnosed with an infection. Due to data limitations, the model's parameters were selected at random, with the most recent influenza data used to establish the assumptions. Simultaneously, we determine the fundamental reproduction number to ensure the system is stable.

Table 2 was used to find that $\mathcal{R}_0 = 4.78 \times 10^{-6}$ which means that the system is stable. Present conditions in Ghana are likely to cause the seasonal inluenza virus, according to our findings ($\mathcal{R}_0 > 1$ in **Table 3**). It is possible that our calculations may not accurately represent the parameter and value of zero because this is a continuous process that is prone to

fluctuations; this is one limitation of our work. In this infographic, we've highlighted how important vaccination patients and programs are for limiting the spread of the seasonal fluvirus in Ghana. The fact that the virus can incubate for a long time, leaving asymptomatic patients, and that it is still potent enough to spread even during this time makes it difficult to discover infected people. Therefore, the only way to make sure that no one gets sick is to put everyone on protection (i.e. Vaccination and quarantine).

Another thing we have noticed is that the rates of recovery for both vaccinated and non-vaccinated individuals help to reduce the infection. From what we can see, our epidemic paradigm was useful in predicting and controlling the seasonal flu outbreak in Ghana. Even limiting our analysis to Ghana, the resulting model and theoretical framework would be useful for any nation. It is our hope that this analysis will help the general population, policymakers, and the government better prepare for and respond to the spread of influenza.

Conflicts of interest

The authors declare that they have no financial or non-financial conflicts of interest related to the work done in the manuscript.

Funding

This research did not receive any specific funding.

References

1- World Health Organization (WHO). [Online] Available : https://www.who.int/news-room/fact-sheets/detail/influenza-(seasonal).

2- World Health Organization (WHO). Available: https://www.afro.who.int/countries/ghana.

3- Xiang Y, Jia Y, Chen L, Guo L, Shu B, Long E. COVID-19 epidemic prediction and the impact of public health interventions: A review of COVID-19 epidemic models. Infectious Disease Modelling 2021; 6:324-342.

4- Pan America Health Organization. Influenza, SARS-CoV-2, RSV and other respiratory viruses. (PAHO) [Online] available at: https://www.paho.org/en/topics/influenza-sars-cov-2-rsv.

5- European Centre for Disease Prevention and Control. Factsheet about seasonal influenza. (ECDC) available at: https://www.ecdc.europa.eu/en/seasonal-influenza/facts/factsheet.

6- National Advisory Committee on Immunization. Canadian immunization guide chapter on influenza and statement on seasonal influenza vaccine for 2016–2017. Ottawa (ON): Public Health Agency of Canada, 2016.

7- European Centre for Disease Prevention and Control. European External influenza virus quality assessment programme. ECDC 2020 data. Stockholm and Copenhagen: European Centre for Disease Prevention and Control and WHO Regional Office for Europe. ECDC and WHO 2022. Contract No.: WHO/EURO:2022-4757-44520-63020.

8- Waldock J, Zheng L, Remarque EJ, Civet A, Hu B, Jalloh SL, et al. Assay harmonization and use of biological standards to improve the reproducibility of the hemagglutination inhibition assay: a FLUCOP collaborative study. Msphere 2021; 6(4): e00567-21.

9- Chen Z, Bancej C, Lee L, Champredon D. Antigenic drift and epidemiological severity of seasonal influenza in Canada. Scientific Reports 2022; 12(1):15625.

10- Brown, Lorena E, and Anne Kelso. Prospects for an influenza vaccine that induces cross-protective cytotoxic T lymphocytes. Immunology and cell biology 2009; 87(4):300-308.

11- Raihen MN, Akter S, Tabassum F, Jahan F, Begum S. A Statistical Analysis of Excess Mortality Mean at Covid-19 in 2020-2021. Computational Journal of Mathematical and Statistical Sciences 2023; 2(2):223-239.

12- Raihen MN, Akter S, Tabassum F, Jahan F, Sardar M. A statistical analysis of positive excess mortality at Covid-19 in 2020-2021. Journal of Mathematics and Statistics Studies 2023; 4(3):07-17.

13- Adekola HA, Adekunle IA, Ekberongbe HO, Onitilo SA, Abdullahi IN. Mathematical modeling for infectious viral disease: The COVID-19 perspective. Journal of public affairs 2020; 20(4): e2306.

14- Adekunle IA, Onanuga AT, Akinola OO, Ogunbanjo OW. Modelling spatial variations of coronavirus disease (COVID-19) in Africa. Science of the Total Environment 2020; 729:138998.

15- Brauer F. Mathematical epidemiology: Past, present, and future. Infectious Disease Modelling 2027; 2(2):113-127.

16- Charlton CL, Babady E, Ginocchio CC, Hatchette TF, Jerris RC, Li Y, et al. Practical guidance for clinical microbiology laboratories: viruses causing acute respiratory tract infections. Clinical microbiology reviews 2018; 32(1):10-1128.

17- Greenberg SB, Krilov LR, Drew WL, Rubin SJ. Cumitech 21, Laboratory diagnosis of viral respiratory disease. Coordinating ed., WL Drew and SJ Rubin. American Society of Microbiology, Washington, DC 1986; 2.

18- Gessner BD, Shindo N, Briand S. Seasonal influenza epidemiology in sub-Saharan Africa: a systematic review. The Lancet infectious diseases 2011; 11(3):223-235.

19- Mahama PN, Kabo_Bah AT, Blanford JI, Yamba EI, Antwi-Agyei P. Reviewing the Past, Present, and Future Risks of Pathogens in Ghana and What This Means for Rethinking Infectious Disease Surveillance for Sub-Saharan Africa. Journal of Tropical Medicine 2022, 2022.

20- World Health Organization (WHO) [Online] available at: FluNet Summary, https://www.who.int/tools/flunet/flunet-summary.

21- Asante IA, Fox AT, Behene E, Awuku_larbi Y, Kotey EN, Nyarko S et al. Epidemiology of influenza in Ghana, 2011 to 2019. PLOS Global Public Health 2022; 2(12): e0001104.

22- Petrova VN, Colin AR. The evolution of seasonal influenza viruses. Nature Reviews Microbiology 2018; 16(1):47-60.

23- Casagrandi, R, Bolzoni L, Levin SA, Andreasen V. The SIRC model and influenza A. Mathematical biosciences 2006; 200(2):152-169.

24- Nigmatulina, KR. Modeling and responding to pandemic influenza: Importance of population distributional attributes and non-pharmaceutical interventions. Diss. Massachusetts Institute of Technology 2009.

25- Murray and James Dickson. An introduction. Heidelberg: Springer 2002.

26- Martcheva M. An introduction to mathematical epidemiology. Vol. 61. New York: Springer 2015.

27- Nishiura H. Correcting the actual reproduction number: a simple method to estimate R 0 from early epidemic growth data. International journal of environmental research and public health 2010; 7(1):291-302.

28- Affi, P. Sensitivity Analysis of the SEIR Epidemic Compartmental Model.

International Journal of Science and Research 2018:352-357.

29- Diekmann O, Heesterbeek JAP, and Roberts MG. The construction of next-generation matrices for compartmental epidemic models. Journal of the royal society interface 2010; 7(47):873-885.

30- Worldometers. [Online]. Available at: https://www.worldometers.info/coronavirus/ .

31- World population review. [Online]. Available at: https://worldpopulationreview.com/.

32- Olaniyi S, Lawal MA, and Obabiyi OS. Stability and sensitivity analysis of a deterministic epidemiological model with pseudo-recovery. IAENG International Journal of Applied Mathematics 2016; 46(2):160-167.

33- Wikipedia. [Online]. Available at: https://en.wikipedia.org/wiki/Demographics_of_Ghana.

34- Ghana Statistical Service (GSS). [online] Available at: https://census2021.statsghana.gov.gh/.

Raihen MN, Ahammed MM, Akter S. Evaluating the impact of seasonal influenza virus: A comprehensive epidemiological forecast and analysis in Ghana from 2021 to 2023. Microbes Infect Dis 2024; 5(2): 463-478.